7. Linear plots of $K_{\text{Al-Si}}$ as a function of $[Al^{3+}]$, consistent with the presence of dinuclear Al (P = 2, Eq. 4) as a small fraction of total Al, were obtained for low (0.11 mM) and high (0.25 mM) $[H_4SiO_4]$ at pH 5.5. From Eq. 4 the slope of these plots is given by

$$m = \Sigma\Sigma K_{2qr}(\tau_3/\tau_{6-q-r})[H_4SiO_4]^{q-1}\{H^+\}^{-(q+r)}$$

Hence, for the case of exclusively one stoichiometry of silica for the dinuclear species, the slope ratio $m' = m_{0\,25}/m_{0\,11}$ is given by the ratio of the two concentrations raised to the $q - 1$ power $(0.25/0.11)^{(q-1)}$ or 2.27 ($q-1$). Values of m' for q = 1, q = 2, and q = 3 are 1, 2.27, and 5.15, respectively. The actual ratio was 1.72 for slope values of $1.8 \times 10^{11} \pm 3.7 \times 10^{10}$ (0.11 mM Si) and $3.1 \times 10^{11} \pm 8.5 \times 10^{10}$ (0.25 mM Si). Theoretically, at least two dinuclear species, including necessarily a 2:1 Al:Si species, would therefore have been present. The silica stoichiometry of the second species was assumed to be 2 by analogy to kaolinite.

8. The 2:1 Al:Si stoichiometry is noteworthy because it is consistent with the stoichiometry of protoimogolite (a positively charged hydroxy-Al-silicate sol) described by Farmer and co-workers as a proposed explanation for the development of the B_s horizon of podzolic soil profiles [V. C. Farmer, J. D. Russel, M. L. Berrow, *J. Soil Sci.* **31**, 673 (1980); V. C. Farmer, *Coloq. Int. CNRS* **303**, 275 (1981); *Soil Sci. Plant Nutr.* (*Tokyo*) **28**, 571 (1982); in *Podzols et Podzolization*, D. Righi and A. Chauvel, Eds. (Assoc. Fr. Estude Sol, Plaisir, France, 1987, pp. 187–194)].

9. The estimates of $K_{(222)}$ and $K_{(212)}$ were generated by simultaneous solution of two equations of the form

$$m_{\{H_4SiO_4\}} = (\tau_3/\tau_3)K_{212}\{H^+\}^{-3} + \tau_3\tau_2K_{222}\{H^+\}^{-4}[H_4SiO_4]$$

where from Eq. 4 the general form of $m_{[H_4SiO_4]}$, given by $\tau_3/\tau_{6-q-r}\Sigma\Sigma K_{2qr}[H_4SiO_4]^{q-1}\{H^+\}^{-(q+r)}$, represents the slope of plots of $K_{\text{Al-Si}}$ as a function of $[Al^{3+}]$ for the case of P = 2. The experimentally determined values of $m_{[H_4SiO_4]}$ for 0.11 and 0.25 mM $[H_4SiO_4]$ were $1.8 \times 10^{11} \pm 3.7 \times 10^{10}$ and $3.1 \times 10^{11} \pm 8.5 \times 10^{10}$, respectively.

10. We have a poor understanding of the kinetic and thermodynamic characteristic of polynuclear OH-Al ions, and little is known of low-order species such as dinuclear OH-Al ions. Compositions and structures remain controversial [P. H. Hsu, in *Minerals in Soil Environments* (Soil Science Society of America, Madison, WI, 1989), pp. 331–378; P. M. Bertsch, *Soil Sci. Soc. Am. J.* **51**, 825 (1987)], and widely varying rates of hydrolysis and nucleation of Al^{3+} have been reported in response to different solution conditions. Most laboratory studies have been conducted at high Al^{3+} concentrations, which tend to obscure the reactions of low-order polynuclear OH-Al ions, and Bertsch has shown that the observed distributions of Al between mononuclear and polynuclear forms are artifacts of synthesis conditions.

11. H. M. May, D. G. Kinniburgh, P. A. Helmke, M. L. Jackson, *Geochim. Cosmochim. Acta* **50**, 1677 (1986). The kaolinite samples studies by May *et al.* were from Dry Branch, GA. Of the smectite samples they studied, two (Upton, WY, and Panther Creek, MO) were from commercial bentonite deposits and the remaining three (Kokokahi, Lualualei, and St. Louis Heights) were samples of the A horizons from Hawaiian Vertisols.

12. We conducted similar calculations for the data of May *et al.* (*11*) on smectite suspensions at pH 6 and 7 but obtained little effect. This result is not surprising because $Al(OSi(OH)_3)^{2+}$ and the dinuclear hydroxy-Al-silicates are unable to compete with OH-Al ions at these pH values. Other soluble hydroxy-Al-silicates may exist that could improve the conformance of the data of May *et al.* (*11*) to smectite phase boundaries at these pH values. However, additional studies are needed to characterize their stoichiometry and stability.

13. Similar implications may apply for the interpretation of weathering experiments. One could propose that the nonstoichiometric release of Al and Si observed in several recent experiments on the dissolution of silicates [L. Chou and R. Wollast, *Geochim. Cosmochim. Acta* **48**, 2205 (1984); G. R. Holdren and R. A. Berner, *Am. J. Sci.* **285**, 994 (1985)] may reflect the stoichiometry of undetected soluble polynuclear Al-Si species. For example, a 2:1 (Al:Si) soluble Al-Si species formed in or released to solution could result in an apparent stoichiometric excess of Al over silica in the solution phase and a layer enriched in silica on the surface of the mineral.

14. It is implicit in congruent and incongruent dissolution models of aluminosilicate minerals that dissolution reactions proceed directly to Al^{3+} without soluble Al-Si intermediates. Such intermediate species could have important roles in mineral transformation or neoformation reactions.

15. Relations between solid Al-Si species and their soluble Al-Si alteration products may be fundamental features of weathering mechanisms. Summary discussions of current perspectives on weathering mechanisms are given by P. R. Bloom and A. E. Nater [in *Rates of Soil Chemical Processes, SSSA Special Publication 27*, D. L. Sparks and D. L. Suarez, Eds. (Soil Science Society of America, Madison, WI, 1991), chap. 7]; S. M. Colman and D. D. Dethier [in *Rates of Chemical Weathering of Rocks and Minerals*, S. M. Colman and D. D. Dethier, Eds. (Academic Press, New York, 1986), pp. 1–20]; and J. Schott and J. C. Petit [in *Aquatic Surface Chemistry*, W. Stumm, Ed. (Wiley, New York, 1987), pp. 293–315].

16. This work was supported by a Presidental Young Investigator Award to C.T.D. Funds were provided by the National Science Foundation, the Empire State Electric Energy Research Corporation, and the Electric Power Research Institute. This is a contribution of the Hubbard Brook Ecosystem Study.

7 February 1992; accepted 27 April 1992

Morphological Disparity in the Cambrian

Derek E. G. Briggs, Richard A. Fortey, Matthew A. Wills

An analysis of the range of morphology among arthropods demonstrates that disparity among living arthropods is similar to that in Cambrian arthropods. The range of morphological design resulting from the Cambrian "explosion" has been overestimated, reflecting a tendency to separate as "problematic" taxa that cannot be accommodated in the classification on the basis of the living biota. Problematic taxa are largely an artifact of an inadequate taxonomy. Special evolutionary processes may not be necessary to explain the early radiation of the metazoans.

Early metazoan fossils that preserve nonmineralized tissues, such as those of the Middle Cambrian Burgess Shale (*1*), include a range of animals that do not fit readily into higher taxa that are based on the living fauna. This has led to claims about the special place of Cambrian organisms in metazoan history, including the assertion that among the Cambrian faunas are many representatives of higher taxa—even "phyla"—that no longer survive (*2*) and that the variety of different body plans was much more extensive in the Cambrian than it is now (*3*). This range of design is termed "disparity" to distinguish it from "diversity," which is measured as number of species or genera (*3*, *4*). There is ample evidence that the Cambrian animals appeared within a relatively short interval of geological time. Thus, the question of whether they show greater disparity than living faunas has important implications for our interpretation of rates of morphological change during the Cambrian. It has been argued, for example, that special genetic mechanisms would have been necessary to achieve what appear to be high degrees of disparity (*3*, *5*).

The arthropods are the most important group in the Burgess Shale in terms of numbers of genera and of individuals (*6*). They are complex enough and preserve sufficient characters to provide credible comparisons with living representatives. Few arthropods from Burgess Shale–type faunas can be assigned readily to one of the four major groups: the Crustacea, Chelicerata, Uniramia, and the extinct Trilobita (*7*). Over 20 genera lack the diagnostic characters of these groups and have therefore been termed problematica. The suggestion that these problematica represent at least 20 unique designs equivalent in rank to the crustaceans, chelicerates, uniramians, and trilobites (*3*) has been a linchpin in models of enormous Cambrian disparity.

Disparity is a difficult concept to define in quantitative terms. Multivariate morphometric assessments of shape or change in shape (*8*) provide the most objective measure. Such an approach has demonstrated that both morphologic dispersion and distinctness of suprageneric taxa (superfamilies) of trilobites increased from the Cambrian to the late Ordovician (*9*). Likewise, morphologic diversity of the blastoid echinoderms essentially increased to the Permian, when they became extinct, in

---

D. E. G. Briggs and M. A. Wills, Department of Geology, University of Bristol, Wills Memorial Building, Queen's Road, Bristol BS8 1TR, United Kingdom.
R. A. Fortey, Department of Palaeontology, Natural History Museum, Cromwell Road, London SW7 5BD, United Kingdom.

spite of an earlier reduction in generic diversity (*10*). But morphometric methods can be used only where an array of point homologies (landmarks) can be recognized in all the forms under comparison or where entire homologous structures are compared (*9–11*). Neither case applies to the Cambrian arthropods. Instead, we used measures based on discretely coded morphological characters. Because there can be no absolute measure of morphologic disparity, one must make relative assessments of its magnitude. Here, we made a comparison between Cambrian and Recent arthropod groups.

Our analyses were based on the 25 Cambrian arthropod taxa preserved in sufficient detail to allow an adequate number of characters to be coded, together with representatives of the 21 main classes or subclasses of Recent arthropods. The living taxa coded were standard textbook examples. This method of sampling Recent forms was preferable to selecting taxa from modern environments similar to those represented by the Burgess Shale and other Cambrian faunas. Many of the ecological niches occupied by arthropods in the Cambrian are now filled by other organisms (*12*), making comparisons inappropriate. The list of morphologic characters is as exhaustive as possible: a total of 134, including those unique to individual taxa (*13*). However, because claims about disparity have been made on the basis of fossil material, only those characters with potential for preservation in a Burgess Shale–type setting were included, thus coding fossil and living forms in an equivalent way.

Fig. 1. Morphological disparity in the Cambrian. Cambrian and Recent arthropods are plotted on the first three principal component axes, which together account for 49% of the total variance. The symbols indicate the score of each taxon on the third principal component axis. Open circles denote negative values. The taxa are joined by a Euclidean minimal spanning tree on the basis of their scores on the first 19 principal components (encompassing 90% of the variance). Recent arthropods are in bold type, and Cambrian arthropods are in italics.

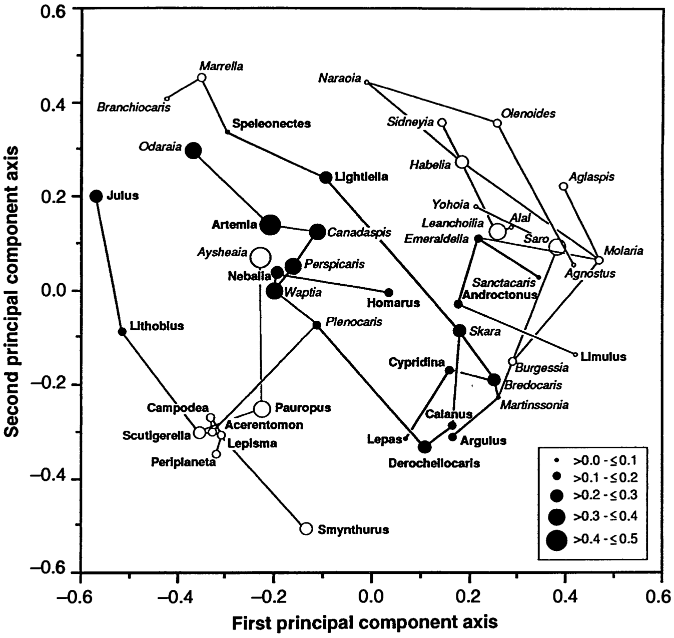

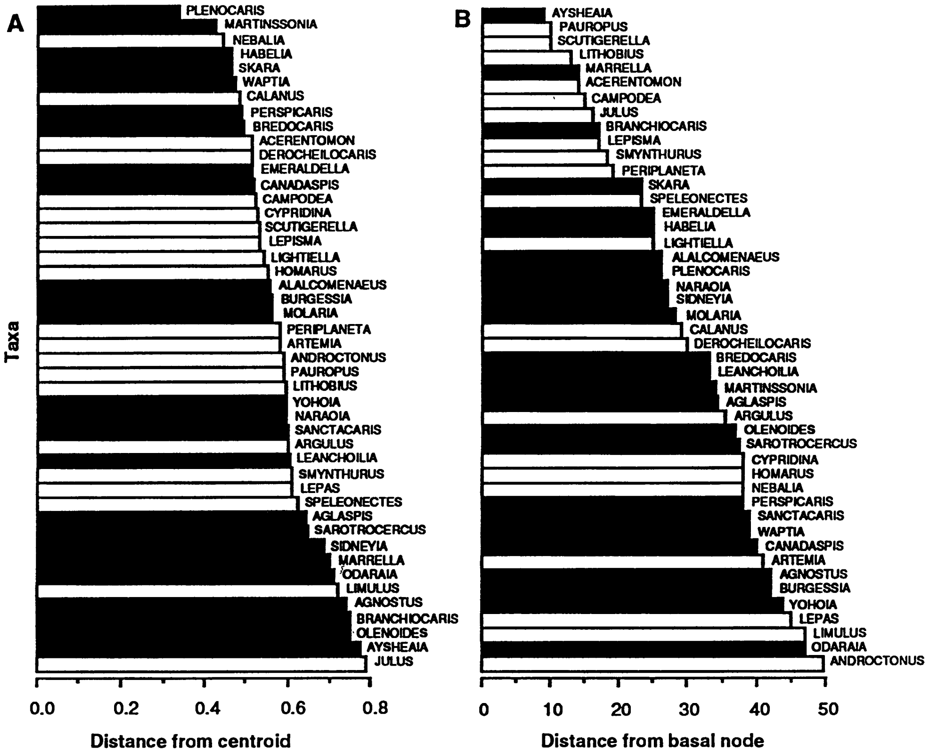

Fig. 2. Histogram of (**A**) Euclidean distances from the centroid of the first 19 principal components (Fig. 1) and of (**B**) distances from the basal node of the cladogram (Fig. 3) to terminal taxa. Each horizontal bar represents one taxon in ascending order of distance from top to bottom. Recent arthropods are unshaded, and Cambrian arthropods are shaded.

To test variation in disparity, we used both phenetic and cladistic approaches as a basis for quantitative treatments. Our aim was to understand disparity, not to analyze phylogeny. Nonetheless, the approaches we adopted are used in phylogenetic analysis. Phenetic methods have been considered an objective measure of relationship because they do not seek to impose a hierarchy based on a polarity of transformation; trees generated by cladistics have been regarded as an approximation to historical reality.

The phenetic approach uses principal component analysis (PCA) based on a covariance matrix, which describes the distribution of the arthropods in morphological hyperspace. (A previous attempt to use PCA to discover relationships among Cambrian arthropods (*14*) was based on fewer characters and did not include Recent taxa.) When a minimal spanning tree (the dendrogram linking nearest neighbors in multidimensional attribute space) is superimposed on a three-dimensional plot, three major groups, the uniramians, the crustaceans, and the "arachnomorphs" (including the chelicerates, trilobites, and related Cambrian genera), separate (Fig. 1). Disparity can be quantified in terms of Euclidean distances from the centroid of this multidimensional space (Fig. 2A). Distances for the Recent arthropods fall among those for the Cambrian taxa, and the distances for the Cambrian arthropods (Table 1) are not significantly different from those of the Recent (Mann-Whitney test).

The taxa are clearly widely scattered in morphospace, but Euclidean distance from the centroid does not incorporate any directional element into the measure of disparity. The amount of morphospace occupied by a particular set of taxa can be represented by the product of the variances or ranges of the scores for these taxa in each of the first 19 dimensions of the PCA plot, which encompasses over 90% of the total variance. Variances have the advantage of being relatively insensitive to sample size, whereas ranges are less influenced by variation in taxonomic practice and therefore might be preferable in this context. The Recent arthropods occupy a volume equal to 89 and 95% of that occupied by the Cambrian arthropods, with variances and ranges, respectively, used (scaled to one dimension) (Table 1).

It might still be argued that the concept of a "body plan" implies that certain characters or character suites are more fundamental than others (*15*), whereas our analysis above incorporates no a priori weighting of morphological attributes. The major taxa of living arthropods, for example, are diagnosed largely on head segmentation. The occurrence of many different arrangements of head segments among the Cambrian arthropods has been used to argue that each represents a fundamentally different ground plan or basic design (*3*). However, previous cladistic analyses have shown that the number of cephalic appendages gives a low consistency index compared to the majority of morphologic characters (*16–18*). Nonetheless, the major groups still emerge from these analyses identified by other morphological characters. Incorporating the acquisition and stabilization of combinations of characters (like head tagmosis) into concepts of disparity implies a phylogenetic interpretation. Cladistics provides an approach to this problem as it identifies a series of character-state transitions delimiting nested sets of taxa.

Table 1. Cambrian disparity.

	Taxa (*n*)	Distance from centroid*	Morphospace occupied: variance/range†	Distance on cladogram‡
Recent arthropods	21	0.574	0.0103/0.401	27.20
Cambrian arthropods	25	0.586	0.0115/0.420	32.40

*Mean Euclidean distance from the centroid of multidimensional attribute space. †Volume of morphospace occupied by different subsets of taxa calculated as the product of the variances and ranges of the scores in each of the first 19 dimensions of the PCA plot that encompasses over 90% of the total variance. ‡Mean distance from the basal node of the cladogram to each terminal taxon (calculated as a mean for the six equally parsimonious solutions).

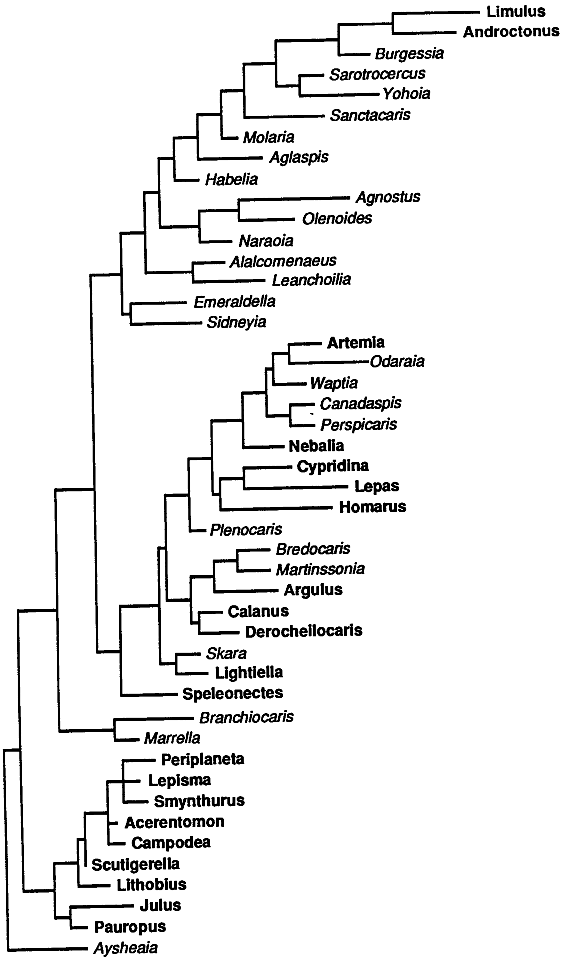

Fig. 3. One of six equally parsimonious phylograms (branch lengths are proportional to the number of character-state transitions along them) for the data set of 46 Cambrian and Recent arthropods. Recent arthropods are in bold type and Cambrian arthropods are in italics.

Our cladistic analysis used the PAUP (phylogenetic analysis using parsimony) program (3.0), which incorporates the minimum possible number of character-state transitions with the conventional criterion of Wagner parsimony. We used a heuristic search, running random addition sequences 200 times and implementing tree bisection-reconnection branch swapping. *Aysheaia* was the designated outgroup. [When the uniramians are omitted, *Marrella* consistently occupies the position at the base of the cladogram (*14, 19*).] Six equally parsimonious solutions resulted, one of which is illustrated here (Fig. 3). Although the general pattern is the same, the cladograms differ in detail from a previous analysis of Cambrian arthropods (*16, 17, 19*) because more living forms, including the uniramians, are added and some new information has been incorporated. The uniramians occupy a primitive position and do not show a relationship to any of the crustaceans. The overall consistency index is 0.268 (excluding cladistically uninformative characters).

The number of character transitions involved in the acquisition of a particular morphology from an ancestral form provides a measure of disparity that can be quantified as the distance between the basal node of the cladogram and the terminal taxon. The result is formulated within the constraints of the cladogram, however, which sequences the acquisition (and loss) of characters to produce a hierarchy of nested sets. Thus, it is a different measure of morphological separation, based on branching order, in comparison to that determined by the phenetic approach (*15*). Although fossil and Recent taxa are clearly interspersed (Fig. 2B), the average distance of the Cambrian arthropods from the base of the cladogram is greater than that of the Recent forms (Table 1). This reflects the concentration of uniramians at a position low in the cladogram.

The analysis of disparity presented here shows that the amount of morphospace occupied by the arthropods of the Cambrian and that occupied by those of the Recent are essentially equivalent. Models of the Cambrian radiation that are based on the premise that problematica should be ranked alongside major living taxa [that is, that the Burgess Shale "contains at least 20 unique designs of arthropods" (*3*) in addition to the four major groups] greatly exaggerate the amount of evolution and extinction required to explain the pattern of events (*17*). Recent descriptions of new discoveries of exceptionally preserved Cambrian fossils (*20*) have led to the reinterpretation of the affinities of other apparently bizarre forms, removing them from the problematica. The recognition of taxa as problematic is a statement of ignorance—an artifact of our level of knowledge and imperfect resolution of relationships. These new discoveries, like the analysis presented here, have damped the Cambrian "explosion." Whereas a morphospace equivalent to that occupied by the range of modern arthropods was filled relatively rapidly, the evidence provides little justification for invoking special evolutionary processes to explain the early radiation of the metazoans.

REFERENCES AND NOTES

1. S. Conway Morris, *Science* **246**, 339 (1989); *Trans. R. Soc. Edinb. Earth Sci.* **80**, 271 (1989).
2. H. B. Whittington, *Proc. Geol. Assoc.* **91**, 127 (1980); *Proc. Linn. Soc. N.S.W.* **105**, 79 (1981); in *Palaeontology: Essential of Historical Geology*, E. M. Gallitelli, Ed. (Mucchi, Modena, Italy, 1982), pp. 11–24; D. E. G. Briggs and S. Conway Morris, in *Problematic Fossil Taxa*, A. Hoffman and M. H. Nitecki, Eds. (Oxford Univ. Press, New York, 1986), pp. 167–183.
3. S. J. Gould, *Wonderful Life: The Burgess Shale and the Nature of History* (Norton, New York, 1989).
4. B. Runnegar, in *Rates of Evolution*, K. S. W. Campbell and M. F. Day, Eds. (Allen & Unwin, London, 1987), pp. 39–60.
5. J. W. Valentine and D. H. Erwin, in *Development as an Evolutionary Process*, R. A. Raff and E. C. Raff, Eds. (Liss, New York, 1987), pp. 71–107.
6. S. Conway Morris, *Palaeontology* (*London*) **29**, 423 (1986).
7. H. B. Whittington, *The Burgess Shale* (Yale Univ. Press, New Haven, CT, 1985), pp. 1–151.
8. D'A. W. Thompson, *On Growth and Form* (Cambridge Univ. Press, Cambridge, 1961).
9. M. Foote, *Syst. Zool.* **39**, 371 (1990); *Palaeontology* (*London*) **34**, 461 (1991).
10. _____, *Univ. Mich. Mus. Paleontol. Contribs.* **28**, 101 (1991).
11. F. L. Bookstein *et al.*, *Acad. Nat. Sci. Philadelphia Spec. Pub.* **15**, 1 (1985).
12. D. E. G. Briggs and H. B. Whittington, *Trans. R. Soc. Edinburgh Earth Sci.* **76**, 149 (1985).
13. The data matrix used in both the phenetic and cladistic analyses can be obtained from the authors.
14. D. E. G. Briggs and H. B. Whittington, *U.S. Geol. Surv. Open-File Rep. 81-743* (1981), pp. 38–41.
15. S. J. Gould, *Paleobiology* **17**, 411 (1991).
16. D. E. G. Briggs and R. A. Fortey, in *Origins and Early Evolutionary History of the Metazoa*, J. W. Lipps and P. W. Signor, Eds. (Plenum, New York, 1992), pp. 335–373.
17. D. E. G. Briggs, in *Arthropod Paleobiology* (*Short Courses in Paleontology*) (Paleontological Society, University of Tennessee, Knoxville, 1990) vol. 3, pp. 24–43.
18. _____, in *Crustacean Phylogeny*, F. R. Schram, Ed. (Balkema, Rotterdam, 1979), pp. 1–22.
19. _____ and R. A. Fortey, *Science* **246**, 241 (1989).
20. S. Conway Morris and J. S. Peel, *Nature* **345**, 802 (1990); L. Ramsköld and H. Xianguang, *ibid.* **351**, 225 (1991).

21. We acknowledge, with thanks, comments and discussion on the quantification of disparity and on phylogenetic analysis from G. A. Boxshall, S. Conway Morris, A. Dennis, S. J. Gould, W. L. Kovach, M. Foote, P. L. Forey, C. Moncrieff, J. M. V. Rayner, J. J. Sepkoski, P. H. A. Sneath, A. Swan, J. T. Temple, and M. Wilkinson. J. W. Archie generously supplied software. M.A.W. was funded by a University of Bristol postgraduate scholarship.

4 February 1992; accepted 29 April 1992

Three-Dimensional Solution Structure of Human Interleukin-4 by Multidimensional Heteronuclear Magnetic Resonance Spectroscopy

Robert Powers, Daniel S. Garrett, Carl J. March, Eric A. Frieden, Angela M. Gronenborn,* G. Marius Clore*

The three-dimensional solution structure of recombinant human interleukin-4, a protein of 133 residues and 15.4 kilodaltons that plays a key role in the immune and inflammatory systems, has been solved by multidimensional heteronuclear magnetic resonance spectroscopy. The structure is dominated by a left-handed four-helix bundle with an unusual topology comprising two overhand connections. The linker elements between the helices are formed by either long loops, small helical turns, or short strands. The overall topology is remarkably similar to that of growth hormone and granulocyte-macrophage colony stimulating factor, despite the absence of any sequence homology, and substantial differences in the relative lengths of the helices, the length and nature of the various connecting elements, and the pattern of disulfide bridges. These three proteins, however, bind to cell surface receptors belonging to the same hematopoietic superfamily, which suggests that interleukin-4 may interact with its receptor in an analogous manner to that observed in the crystal structure of the growth hormone-extracellular receptor complex.

Interleukin-4 (IL-4) is one of a group of cytokines that play a central role in the control and regulation of the immune and inflammatory systems (*1*). Specific activities associated with IL-4 are the stimulation of activated B cell, T lymphocyte, thymocyte, and mast cell proliferation and the induction of cytotoxic $CD8^+$ T cells. The latter is responsible for the antitumor activity of IL-4. Renal tumor cells that secrete large doses of IL-4 can establish tumor-specific immunity toward a preexisting renal cancer (*2*). In addition, IL-4 induces the expression of class II major histocompatibility complex (MHC) molecules and the immunoglobulin E (IgE) low-affinity receptor on resting B cells (*3*). Further, IL-4 is responsible for generating and sustaining in vivo IgE responses and for ensuring the dominance of IgG1 in the T cell–dependent immune response by causing immunoglobulin class switching of activated B cells to IgE and IgG1, respectively (*3*). In order to provide a structural basis for understanding the mode of action of IL-4 and its interaction with its cell surface receptor, we have determined the three-dimensional (3D) structure of human recombinant IL-4 (15.4 kD and 133 residues) in solution using multidimensional heteronuclear NMR (nuclear magnetic resonance) spectroscopy.

The NMR structure determination was principally based on 823 approximate interproton distance restraints derived from 3D ^{15}N- (*4*) and ^{13}C-separated (*5*) NOESY (nuclear Overhauser enhancement spectroscopy) spectra and a ^{1}H-^{15}N HMQC (heteronuclear multiple quantum coherence)–NOESY-HMQC spectrum (*6*) recorded on uniformly (>95%) labeled ^{15}N- and ^{13}C-^{15}N–labeled human recombinant IL-4 (*7, 8*). These spectra were interpreted on the basis of complete ^{1}H, ^{15}N, and ^{13}C assignments obtained previously with 3D double- and triple-resonance NMR spectroscopy (*9*). [Note that a partial set of ^{1}H and ^{15}N assignments has also been published by Redfield *et al.* (*10*)]. An example of the quality of the 3D ^{13}C-separated NOESY spectrum is shown in Fig. 1. The interproton distance restraints were classified into three distance ranges, 1.8 to 2.7 Å, 1.8 to 3.3 Å [1.8 to 3.5 Å for nuclear Overhauser effects (NOEs) involving NH protons], and 1.8 to 5.0 Å, corresponding to strong, medium, and weak NOEs, respectively (*11, 12*). With the exception of sequential $C\beta H(i)$-$NH(i+1)$ NOEs, all NOEs involving side chains were derived from the 3D ^{13}C-separated NOESY spectrum. Although the ^{1}H chemical shift dispersion of IL-4 is small (*10*), the increased resolution afforded by separating the NOEs into a third dimension according to the ^{13}C chemical shift of the carbon atom attached to the destination proton is sufficient to extract a large number of NOEs unambiguously by making use of the symmetry relations inherent to this spectrum. Thus, the NOE from proton *i* to proton *j* is labeled by the ^{13}C chemical shift of the carbon atom attached to proton *j*, and the symmetry-related NOE from proton *j* to proton *i* is labeled by the ^{13}C chemical shift of the carbon atom attached to proton *i*. In this

---

R. Powers, D. S. Garrett, A. M. Gronenborn, G. M. Clore, Laboratory of Chemical Physics, National Institute of Diabetes and Digestive and Kidney Diseases, National Institutes of Health, Bethesda, MD 20892.
C. J. March and E. A. Frieden, Immunex Corporation, 51 University Street, Seattle, Washington 98101.

*To whom correspondence should be addressed.